

## Analysis of Turbulent Mixed Convection Flow in A Ventilated Enclosure

Dr. Adel A. Alwan  
Mech. Eng. Dept.  
College of Engineering  
Babil University

Dr. Alla A. Mahdi  
Mech. Eng. Dept.  
College of Engineering  
Kufa University

Dr. Khudheyer S. Mushatet.  
Mech. Eng. Dept.  
College of Engineering  
Thiagar University

### Abstract

In this work, a numerical study on turbulent mixed convection inside a rectangular enclosure is performed to predict the distribution of air velocity, turbulent kinetic energy, temperature and Nusselt number variation under different locations of supply and return outlets. Four cases were studied with respect to supply outlet and two cases for the return outlet. The effect of Archimedes number and Reynolds number on the turbulent flow and heat transfer characteristics is examined. The Navier- Stokes, energy equations and turbulence equations are solved using finite volume method. The k- $\epsilon$  model with wall function approximations is used to model the turbulence. The obtained results show that the turbulent flow and heat transfer characteristics are noticeably effected with changing the positions of supply and return outlets. The local Nusselt number is increased with the increase of Archimedes number and decreased with the increase of Reynolds number. The validation of the present code is done through a comparison with the available published experimental data.

### المستخلص:

في هذا البحث اجريت دراسة عددية للحمل المختلط الاضطرابي داخل حيز مستطيل وذلك لتخمين سرع الهواء ودرجات الحرارة والطاقة الحركية للاضطراب بالإضافة الى عدد نسلت تحت تاثير مواقع مختلفة من فتحات دخول وخروج الهواء. تم دراسة اربعة حالات بالنسبة لتغير موقع فتحة دخول الهواء وحالتين بالنسبة لتغير موقع فتحة خروج الهواء. تم اختبار تأثير عدد رينولدز وعدد أرخميدس على خصائص الجريان الاضطرابي وانتقال الحرارة. معادلات نافير-ستوكس ومعادلة الطاقة ومعادلات الاضطراب تم حلها باستخدام طريقة الحجم المحدد مع اعتماد تقنية الشبكة الزاحفة. في هذه الدراسة استخدم موديل الاضطراب (k- $\epsilon$ ) لنمذجة الاضطراب مع العلاقات التجريبية لدالة الجدار. اوضحت النتائج التي تم الحصول عليها أن خصائص الجريان الاضطرابي وانتقال الحرارة قد تأثرت بصورة ملحوظة عند تغير مواقع فتحات دخول وخروج الهواء. ايضا بينت النتائج أن عدد نسلت الموضعي قد قل مع زيادة عدد رينولدز وازداد مع زيادة عدد أرخميدس. تم التأكد من سلامة الطريقة العددية المستخدمة من خلال المقارنة مع النتائج العملية المنشورة.

### Nomenclature

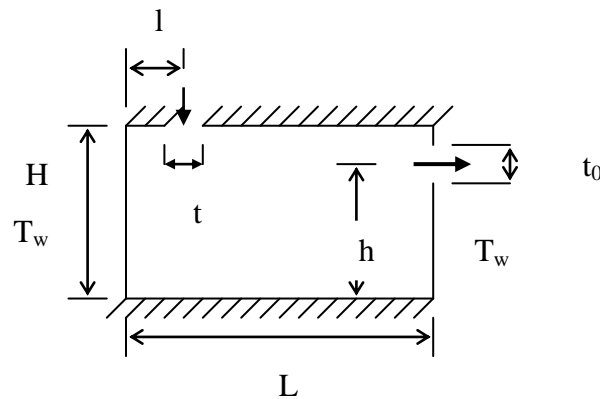
$A_r$	Archimedes number $(Gr/Re^2)$ , -
$Gr$	Grashof number $\left(\frac{\rho g \beta H^3 \Delta T}{\mu^2}\right)$ , -
$H$	height of the enclosure, m
$i, j$	tensor notation, -
$k$	turbulence kinetic energy, $m^2/s^2$
$L$	length of the enclosure, m
$Nu$	local Nusselt number $\left(Nu = -\int_0^1 \frac{d\theta}{dx}\right)$ , -
$p$	pressure, $N/m^2$
$Re$	Reynolds number $\left(\frac{U_{in} t}{\nu}\right)$ , -
$t$	width of supply outlet, m
$t_o$	width of return outlet, m
$T$	temperature, $^{\circ}C$
$T_{in}$	supply outlet temperature, $^{\circ}C$
$T_w$	wall temperature, $^{\circ}C$
$U_{in}$	inlet velocity at a supply outlet, m/s
Greek symbols:	
$\epsilon$	turbulence dissipation rate, $m^2/s^3$
$\mu$	molecular viscosity, $N.s/m^2$
$\nu_t$	eddy viscosity, $m^2/s$
$\sigma_k ; \sigma_{\epsilon}$	turbulent schmidt numbers, -
$S_{\phi}$	source term, -
$\theta$	dimensionless temperature, -

### 1. Introduction

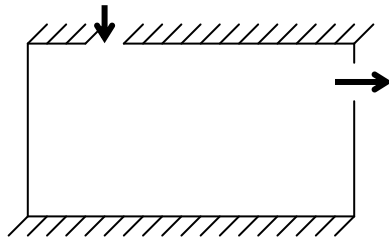
Indoor environment design requires a detailed information about the flow and heat transfer characteristics besides to the pollutant concentrations. There are two main ways to obtain the characteristics of air flow inside the enclosure, one from full-scale test and the other from numerical analysis. Some papers have been published on the experimental investigation of indoor air motion [1,2]. Such investigations are expensive and detailed measured data are not available. Nielson [3] simulated numerically the two dimensional turbulent air flow in rooms using stream function-vorticity approach along with a k- $\epsilon$  turbulence model proposed by Gosman et al. [4]. A reasonable air flow distribution plays a significant role in obtaining satisfied indoor environment. An interesting review on the application of

computational fluid dynamics in a ventilated rooms was given by Awbi [5]. Sinha et al. studied the two dimensional room air flow with and without buoyancy [6]. Lee et al. [7] applied finite volume element method to study the characteristics of forced mixed convection in air cooled room for both laminar and turbulent regimes. Mark [8] studied numerically the three dimensional non-isothermal flow in a mechanically ventilated plenum positioned above a ceiling and extracted across the whole of the floor. Also Guanghbei et al. [9] predicted the isothermal turbulent flow in a rectangular room using 2D and 3D (k- $\epsilon$ ) model. The steady of two and three dimensional laminar and turbulent non-isothermal flow in a room was studied by Gosman [10].

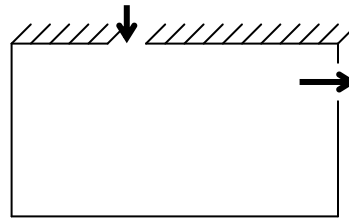
In this work, a two dimensional mixed convection turbulent flow inside an enclosure is studied numerically under different positions of supply and return outlets as shown in Fig.1. The non-isothermal supply temperature is ranged from 14 °C to 23 °C, the Reynolds number from 1429 to 3568 while the Archimedes number from 0.2 to 3.2. The simulated problem is approached to a full scale room (3.5m×2.5m). Six cases were examined regarding the positions of supply and return outlets under different supply temperature and velocities. The governing equations of turbulent mixed convection are solved using finite volume method along with a staggered grid techniques. The aim of the present study is predict the turbulent flow and heat transfer characteristics inside a ventilated enclosure with non-isothermal air supply temperature under different positions of supply and return openings consequently obtaining the best studied case.



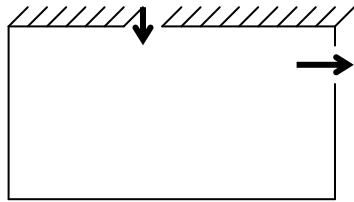
a. case (1),  $l/L=0.1$ ,  $h/H=0.85$ ,  $t=0.1L$ ,  $t_0=0.1H$



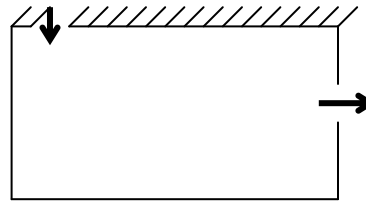
b. case (2),  $l/L=0.15$ ,  $h/H=0.85$



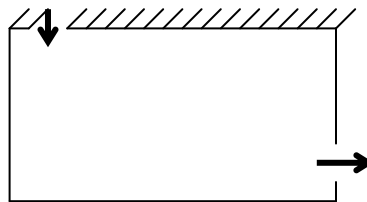
c. case (3),  $l/L=0.25$ ,  $h/H=0.85$



d. case (4),  $l/L=0.35$ ,  $h/H=0.85$



e. case (5),  $l/L=0.1$ ,  $h/H=0.5$



f. case (6),  $l/L=0.1$ ,  $h/H=0.1$

Fig.1. Schematic diagram of the considered problem.

## 2. Mathematical Model.

The instantaneous motion of turbulent flow can be mathematically solved using the conservation laws of mass and momentum. More than 250 years ago, Claude Navier and George Stokes derived the differential equations that govern the behavior of fluid mechanics [3]. These equations are the conservation laws of momentum and the instantaneous turbulent flow field. The general form of these governing equations can be written as follows[3]:

Continuity equation

$$\frac{\partial}{\partial x_i} (\rho u_i) = 0 \text{-----(1)}$$

momentum equation:

$$\frac{\partial \rho \tilde{u}_i \tilde{u}_j}{\partial x_j} = \frac{-\partial \tilde{p}}{\partial x_i} + \frac{\partial}{\partial x_j} \left( \mu \frac{\partial \tilde{u}_i}{\partial x_j} \right) \text{-----(2)}$$

The instantaneous quantity  $\tilde{\phi}$  can be expressed as  $\tilde{\phi} = \bar{\phi} + \phi'$ , where  $\bar{\phi}$  is the time averaged value and  $\phi'$  is the fluctuation part of  $\tilde{\phi}$ . After Reynolds averaging the governing equations and using the above expression of the instantaneous quantities, the equations have the following form:

$$\frac{\partial}{\partial x_i} (\rho U_i) = 0 \text{-----(3)}$$

$$\frac{\partial \rho U_i U_j}{\partial x_j} = \frac{-\partial P}{\partial x_i} + \frac{\partial}{\partial x_j} \left( \mu \frac{\partial U_i}{\partial x_j} - \overline{\rho u_i u_j} \right) + \rho g \beta (T_j - T_{in}) \text{-----(4)}$$

$$\frac{\partial \rho U_i T_j}{\partial x_j} = \frac{\partial}{\partial x_j} \left( \frac{\mu}{Pr} \frac{\partial T_i}{\partial x_j} - \overline{\rho u_i t_j} \right) \text{-----(5)}$$

Where  $\overline{\rho u_i u_j}$  constitute the second – moments statistical correlation or so-called Reynolds stresses.  $\overline{\rho u_i t_j}$  are called turbulent heat fluxes.

## 2-1 Turbulence Model

One of the most widely spread models is the standard k-ε model used by Launder and Spalding [11]. This model applies two transport equations, one for turbulent kinetic energy and the other for the dissipation rate of turbulent kinetic energy as follows:

$$\frac{\partial \rho k U_i}{\partial x_j} = \frac{\partial}{\partial x_j} \left[ \left( \mu + \frac{\mu_t}{\sigma_k} \right) \frac{\partial k}{\partial x_j} \right] + \rho (P_k - \varepsilon) \text{-----(6)}$$

$$\frac{\partial \rho \varepsilon U_j}{\partial x_j} = \frac{\partial}{\partial x_j} \left[ \left( \mu + \frac{\mu_t}{\sigma_\varepsilon} \right) \frac{\partial \varepsilon}{\partial x_j} \right] + \rho \frac{\varepsilon}{k} (C_{1\varepsilon} P_k - C_{2\varepsilon} \varepsilon) \text{-----(7)}$$

where the shear production term, ( $P_k$ ) are define as:

$$P_k = \nu_t \left( \frac{\partial u_i}{\partial x_j} + \frac{\partial u_j}{\partial x_i} \right) \frac{\partial u_i}{\partial x_j} \text{-----(8)}$$

and the eddy viscosity is define as:

$$\nu_t = \rho C_\mu \frac{k^2}{\varepsilon} \text{-----(9)}$$

the model coefficients are ( $\sigma_k$  ;  $\sigma_\varepsilon$  ;  $C_{1\varepsilon}$  ;  $C_{2\varepsilon}$  ;  $C_\mu$ ) = (1.0 , 1.3 , 1.44 , 1.92, 0.09 ) respectively[11]. These coefficients are considered empirical coefficients.

## 2-1 Boundary Conditions:

In order to complete the mathematical model , the following boundary conditions are defined as follows according to Ref.[5]

At supply outlet

$$U = U_{in}$$

$$k = 0.05 U_{in}^2$$

$$\epsilon = k^{1.5} / \lambda t$$

$$\lambda = 0.05$$

At return outlet, normal gradients are imposed

at the walls, no slip boundary conditions( $u = v = 0$ ) are imposed.

To capture the steep gradients near the wall region, a wall function approximation used by Versteeg [12] is adopted here.

### 3- Numerical Procedure

Finite volume method (FVM) is used to solve the above mentioned mathematical model. This gives a system of discretisation equations which means that the system of elliptic partial differential equations is transformed to the system of algebraic equations. Common Gauss-Siedl method helps in solving algebraic equations system. The essence of the discretization is to select appropriate discretization scheme (appropriate option of balance between convective and diffusion terms through the boundary of each control volume.) The general governing differential equations takes the form[12]:

$$\text{div}(\rho U \Phi) = \text{div}(\Gamma \text{grad} \Phi) + S_{\Phi} \quad (9)$$

In this paper orthogonal grid with hybrid scheme is used. The one dimensional convective and diffusive fluxes can be expressed as follows:

$$J_x = \rho U \Phi - \Gamma \frac{\partial \Phi}{\partial x} \quad (10)$$

Then by using finite volume method the discretization of east side flux by hybrid scheme gives the form [12]:

$$\left( \rho U \Phi - \Gamma \frac{\partial \Phi}{\partial x} \right)_e = (\rho U)_e \frac{\Phi_p + \Phi_e}{2} - \Gamma_e \frac{\Phi_p + \Phi_e}{\Delta x_e} \quad (11)$$

A computer program is built using Fortran language to obtain the results of numerical procedure using SIMPLE algorithm. The first calculation is started from zero field and the every one takes the previous as initial condition.

### 4. Results and Discussion

The results obtained from this study including velocity vectors, temperature distribution, turbulent kinetic energy and total Nusselt number are discussed as follow:

Fig.2., case(1) demonstrates the computed velocity vectors for different values of Archimedes number and constant supply velocity ( $Re = 1429$ ). It can be seen that when the temperature difference increase (i.e. increasing  $A_r$ ), the velocity components values are increased because of the increase of buoyancy forces. The boundary layers are formed in the vicinity of the walls while there is nearly stagnant core region in the middle of the enclosure. This stagnant region seems to be larger at the lower Archimedes number ( $A_r = 1.25$ ). However the general flow structure is similar. Also for the case one, when the Reynolds number increasing, the values of

the velocity components increase and when Reynolds number exceeds 3000 (Fig.3.) the flow behavior is noticeably changed. The boundary layer seems to be thicker at the lower wall. This situation is close to the forced convection flow. However the semi stagnant core region is still formed. The stream lines for different Reynolds numbers are depicted in Fig.4. This Figure gives us an obvious verification of what we have discussed above. The stream lines are close to each other at the lower wall for  $Re=3563$ . The effect of changing the position of the supply outlet on the flow distribution is seen in Fig.5. As the figure shows, there is significant changes in the flow recirculation, boundary layers and position of semi- stagnant core . In (a), the flow re-circulates near the supply outlet and the boundary layer seems to be thicker at the left and the bottom wall. There is a start of re-circulation between the supply outlet and the left wall. However this re circulation is small. It is expected, this case is not favorable to dilute concentration if exists and also from the required air distribution and thermal comfort. Therefore a short circuit phenomena is not favorable from the design side. In (b), a new recirculation region is formed between the supply outlet and the left wall and the central core region creeps to the left side. The boundary layer thickness on the wall is closer to the case (1). In (c), central core region is seem to be closure to the left side and in the same time it is smaller in size compared with (a) and (b). It is evident that the values of the velocity vectors are large close to the left and upper wall. The effect of changing the position of the return outlet on the flow distribution is demonstrated in Fig.6(b and c). It is clear that the flow structure are dramatically changed when the return outlet is shifted from the upper right corner. In (b), the stagnant core region becomes larger but the inertia of the flow is decreased noticeably at the upper half of the enclosure. The velocity vector values is larger in the vicinity of the left and bottom wall. The central core region is seem to be larger at case (6). The boundary layer is thicker at the right wall and upper wall. Fig7. exhibits the distribution of turbulent kinetic energy for different values of Reynolds number. It can be seen that the turbulent kinetic energy increases with increasing Reynolds number. The temperature distribution for different values of supply outlet velocity is shown in Fig.8. As the figure shows, there is increase in temperature values with the increase or Reynolds number. The variation of local Nusselt number with Archimedes number is shown in Fig.9. It can be seen that the local Nu is a little increased with the increase of  $A_r$ . The variation of local Nu for the considered cases is depicted in Fig.10. It is evident that the case (1) gives the high Nusselt number followed by a case (6) and case (5). The local nusselt number for all the studied cases is decreased with the increase of the Reynolds number as shown in Figs.(10-11). The present computed results are compared with available published experimental data as shown in Fig.12. The comparison indicated acceptable agreement.

### 5. Conclusion

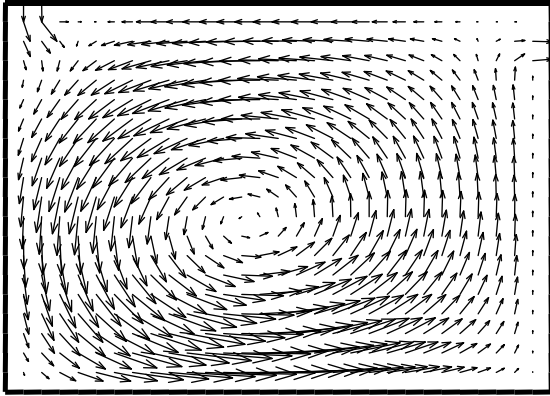
1. The k- $\epsilon$  turbulence model is successfully used to simulate the turbulent mixed convection flow inside an enclosure which approximated to full-scale room under different positions of supply and return outlet.
2. Among the six studied cases, case (1) can give the best air distribution and thermal performance.

- 3. For all the studied case, the local Nusselt number is slightly increased with the increase of the Archimedes number.**

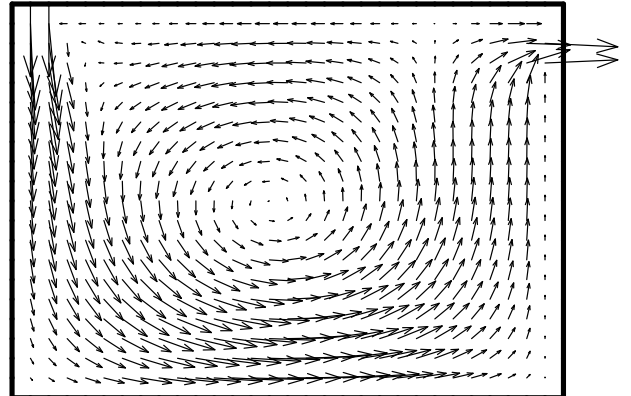
### **References**

1. Nielson, A., Olson, E., "Measurements of air change and energy loss with large open out doors", Building and Physics, Denmark, 1993.
2. Kiel, D.E, Wilson, D.J., " Garvity driven flows through open doors", 7<sup>th</sup> AIC Upou, UK, 1986.
3. Nielson, P.V., " Flow in air conditioning rooms", PhD thesis, Tech. Univ. of Denmark
4. Gosman, A.D., Pun, W.M, Runchal, A.K., Spalding, D.B, " Heat and mass transfer in Re-circulating flows", Academic press, London, 1969.
5. Awbi, H., " application of computational fluid dynamics in room ventilation", Building and Environment", 1989.
6. Sinha, S.L., Arora, R., Roy, S., "Numerical simulation of two dimensional room air flow with and without buoyancy", Energy and Building, 2000.
7. Lee, S.C., Cheng, C.Y., " Finite element solutions of laminar and turbulent flows with forced and mixed convection in an air cooled room", Numerical Heat Transfer, part A31, 1997.
8. Mark, J., " Practical air flow design and optimization in clean rooms using mathematical modeling", England, 2003.
9. Guangbei, Tu, Wenhao Chen, Lai Wang, "Study on flow of clean room", Tianjin University, RR. China, 2003.
10. Basman Al-Hadidi, " Computational study of flow in mechanically ventilated space", 7<sup>th</sup> conference of fluid dynamics and propulsion", December, Sharm El-Sheikh, Egypt, 2001.
11. Launder, B.E., Spalding, D.B, " Lectures in Mathematical model of turbulence, Academic Press, London and New York, 1972.
12. Versteeg, H. and Meer, W., " An Introduction of Computational Fluid Dynamics", Hemisphere Publishing Corporation, United State of Americas.
13. Jones, P. J., Whittle, G. E., "Comptational fluid dynamics for building air flow prediction- current status and capabilities", Building and Environment, 1993.

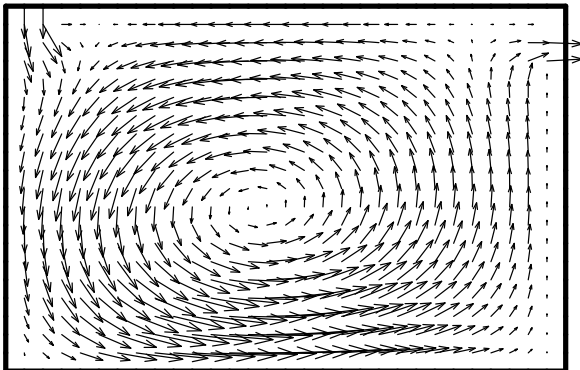




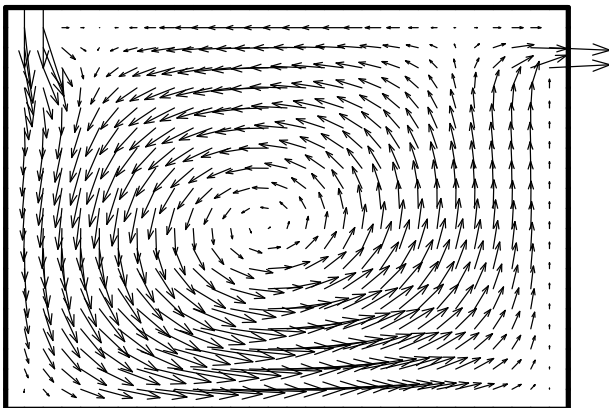
a.  $Re=1429$ ,  $\Delta T=7$ ,  $Ar=3.5$



d.  $Re=3563$ ,  $\Delta T=7$ ,  $Ar=0.2$

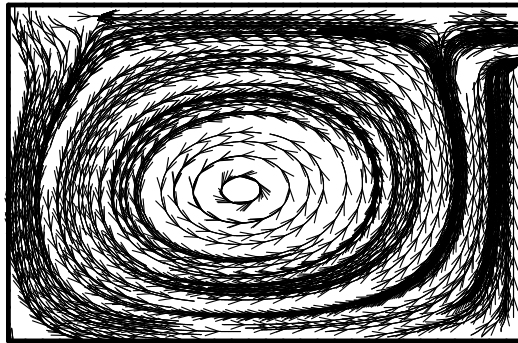


b.  $Re=2141$ ,  $\Delta T=7$ ,  $Ar=2.19$

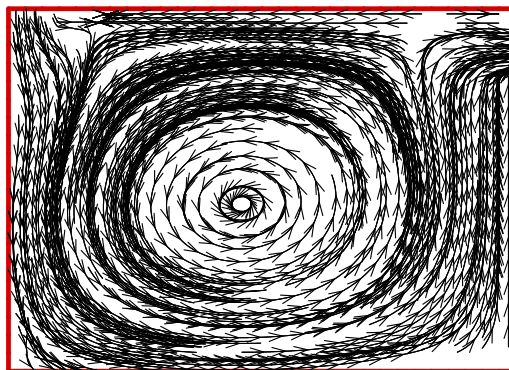


c.  $Re=3000$ ,  $\Delta T=7$ ,  $Ar=0.8$

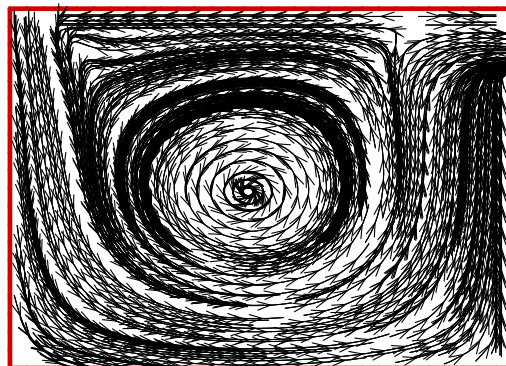
Fig.3 effect of Reynolds number on the computed flow field, case(1).



a.  $Re=1429$ ,  $\Delta T=7$ ,  $Ar=2.19$

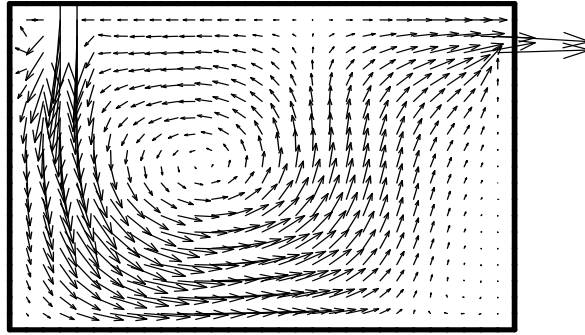


b.  $Re=2141$ ,  $\Delta T=7$ ,  $Ar=0.8$

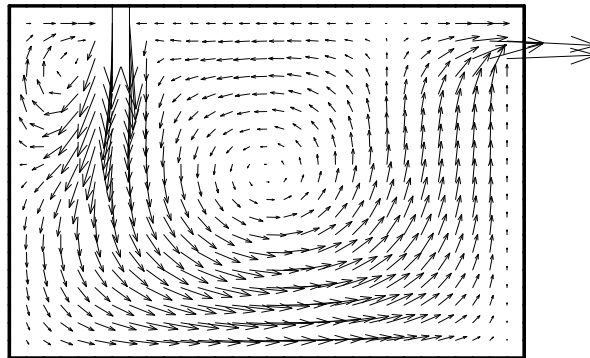


c.  $Re=3563$ ,  $\Delta T=7$ ,  $Ar=0.2$

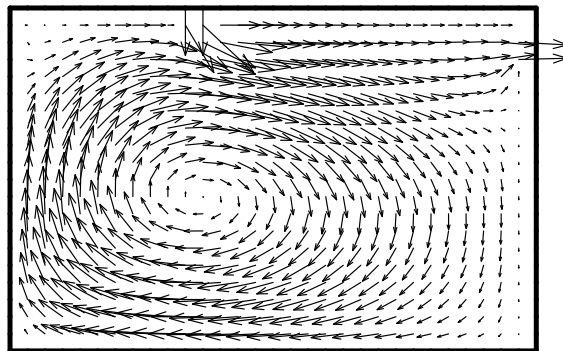
Fig.4 predicted stream lines for different Reynolds numbers, case (1).



a. case(2),  $Re = 3563$ ,  $\Delta T = 7$ ,  $Ar = 0.2$

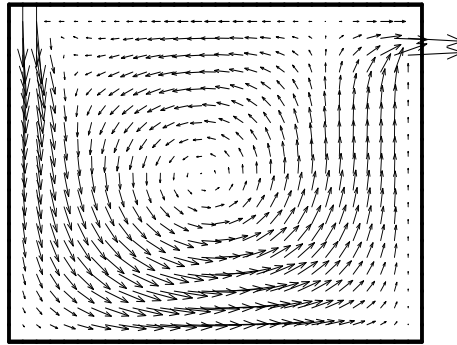


b. case(3),  $Re = 3563$ ,  $\Delta T = 7$ ,  $Ar = 0.2$

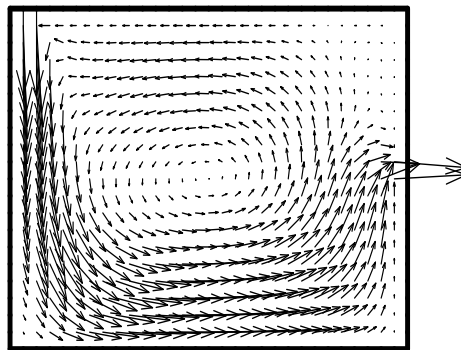


c. case(4),  $Re = 3563$ ,  $\Delta T = 7$ ,  $Ar = 0.2$

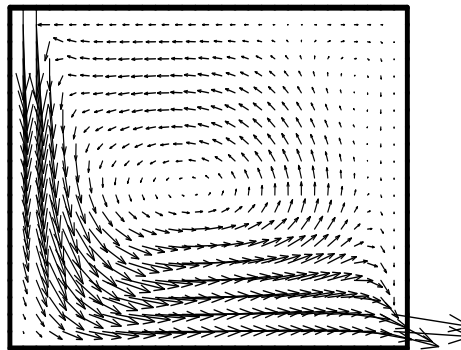
Fig.5 flow field for different positions of supply outlet.



a. case(1),  $Re = 3563$ ,  $\Delta T = 7$ ,  
 $Ar = 0.2$

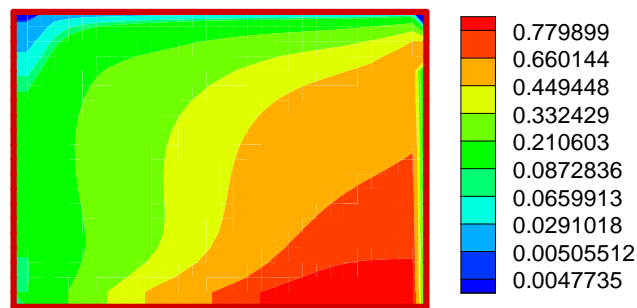


b. case(5),  $Re = 3563$ ,  $\Delta T = 7$ ,  $Ar = 0.2$

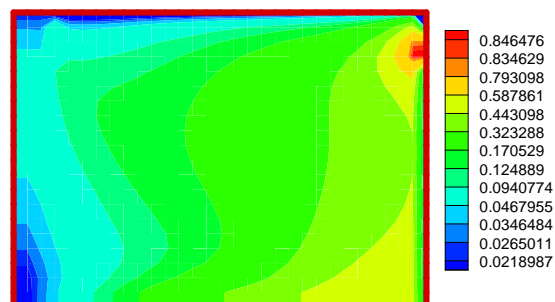


c. case(6),  $Re = 3563$ ,  $\Delta T = 7$ ,  
 $Ar = 0.2$

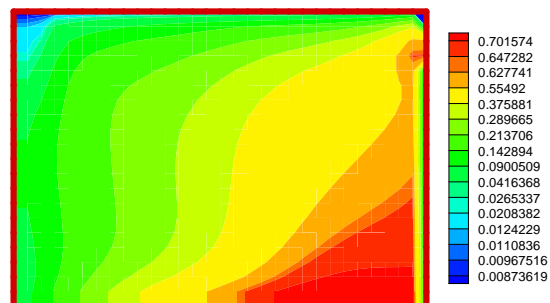
Fig.6. flow field with different positions of return outlet



a.  $Re=1429$ ,  $\Delta T=7$ ,  $Ar=2.19$

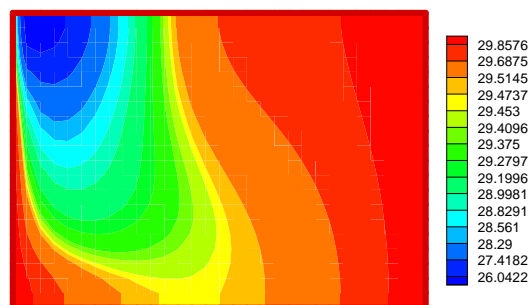


b.  $Re=2141$ ,  $\Delta T=7$ ,  $Ar=0.8$

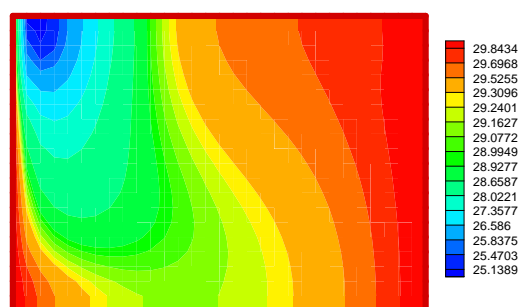


c.  $Re=3563$ ,  $\Delta T=7$ ,  $Ar=0.2$

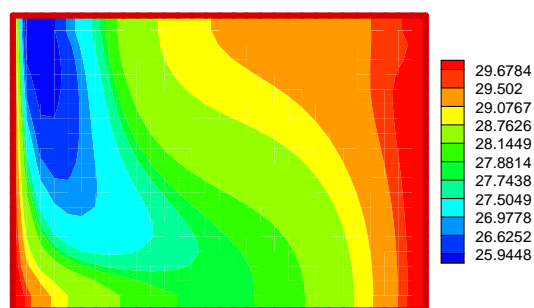
Fig.7 contours of predicted turbulent kinetic energy, case(1).



a.  $Re=1429$ ,  $\Delta T=7$ ,  $Ar=2.19$



b.  $Re=2141$ ,  $\Delta T=7$ ,  $Ar=0.8$



c.  $Re=3563$ ,  $\Delta T=7$ ,  $Ar=0.8$

Fig.8. temperature field with different supply outlet velocities, case(1).

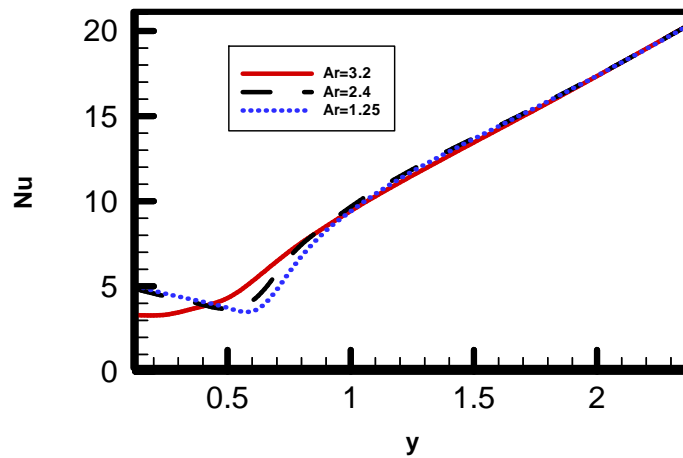


Fig.9. effect of Archimedes number on Nu variation along left wall for the case (1),  $Re=1429$ ,  $Ar=3.2$

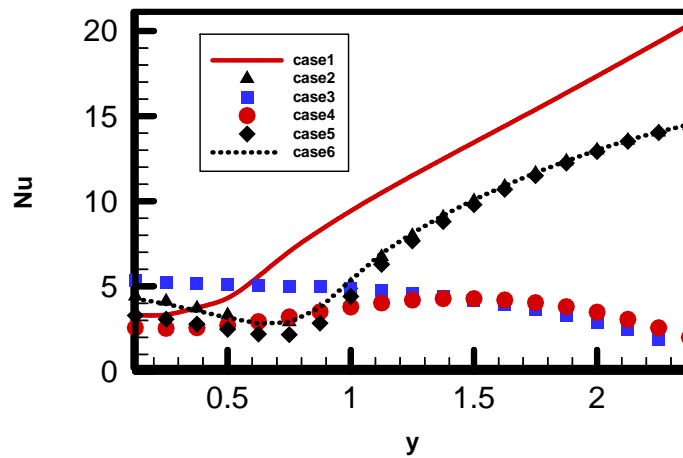
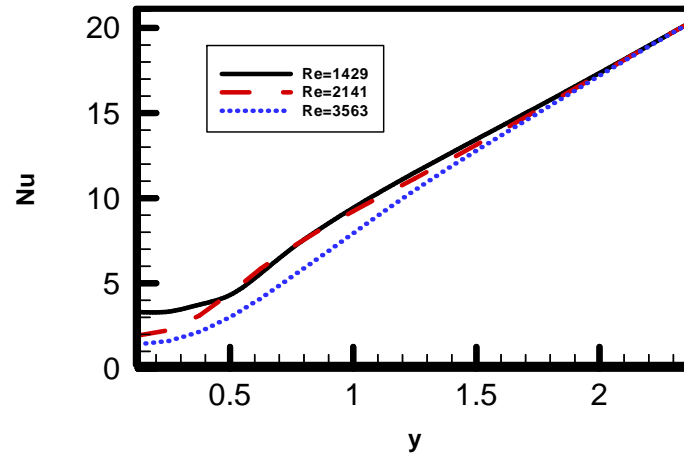
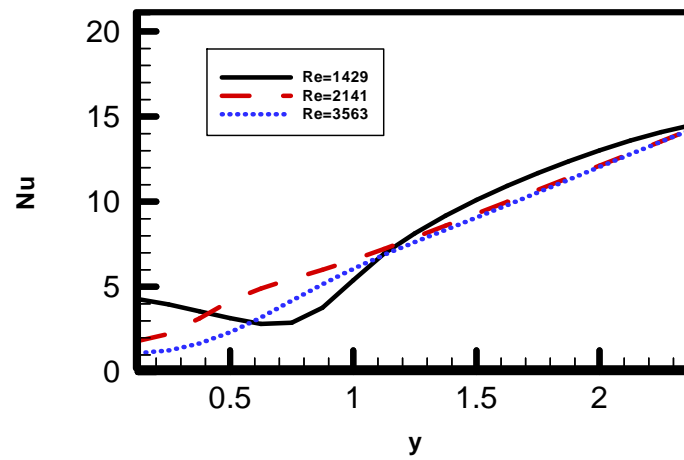


Fig.10. Nu variation along the left wall for the considered cases,  $Ar=3.2$ ,  $Re=1429$



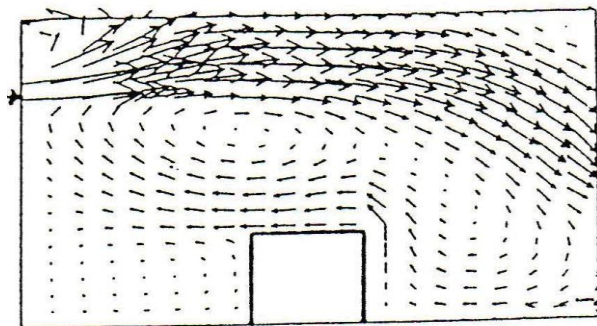
a. case (1).



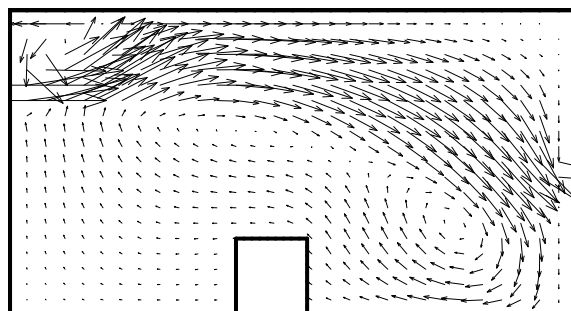
b. case (6).

Fig.11. effect of Reynolds number on Nu variation along left wall, Re=1429





a. Experiments[13]



b. present prediction

Fig.12. comparison between present and published results